DOI: 10.2507/34th.daaam.proceedings.xxx

ROBOTIZATION OF IN-ORBIT LARGE-SCALE STRUCTURE ASSEMBLY

Vladislav Kopylov, Igor Shardyko* & Victor Titov

This Publication has to be referred as: Kopylov, V[ladislav]; Shardyko, I[gor] & Titov, V[ictor] (2023). Robotization of In-Orbit Assembly Large-scale Structure Assembly, Proceedings of the 34th DAAAM International Symposium, pp.xxxx-xxxx, B. Katalinic (Ed.), Published by DAAAM International, ISBN 978-3-902734-xx-x, ISSN 1726-9679, Vienna, Austria
DOI: 10.2507/34th.daaam.proceedings.xxx

Abstract

Large-scale spacecraft structures provide the better part of the critical features of a satellite. The increase in size of the structures leads to a greater power reserve, an increased number of relay channels, better resolution quality, and so on. Nowadays, deployable from folded-state structures have reached the technological limits of their own size. In order to overcome these limits, it is often proposed to assemble space structures directly in space. However, a lot of issues remain that need a feasible and efficient solution. In this article, the key aspects of in-orbit robotic assembly technology are discussed, such as the technology of mechanical connections, robotic motion and operation performance, and the overall layout of the space structure. Then special attention is paid to the mathematical model that is necessary to build the control system, whose basic design is also proposed. The total concept makes it possible to assemble large-scale structures providing oscillation damping relying upon existing spacecraft control system capabilities.

Keywords: robotic assembly; large-scale space structures; spacecraft; solar panels; truss structures.

1. Introduction

In-orbit assembly of large-scale structures gives huge advantages that were clear from the origin of the space industry. Assembly operations have been tested in all EVA missions since the first spacewalk (A. Leonov mounted a TV camera to the spacecraft outer surface). The most significant work was carried out on the space stations. Namely, due to the assembly in space, it has become possible to achieve the unprecedentedly big power reserve of the ISS provided by the ITS-truss with solar panels and radiators installed on it [1]. However, the ITS-truss itself was delivered in the cargo bay of a space shuttle that was already assembled. Nowadays, it is not possible to repeat such an assembly as no means of delivery exist that could provide sufficient payload volume.

The experiments “Sophora”, “Rapana”, and “Strombus”, conducted from 1991 to 1996 on the Mir space station [2], have shown the fundamental possibility of assembling a sufficiently precise and stable truss mast from short segments directly on the orbit. All these experiments assumed the participation of a cosmonaut to perform each connection, which means high labour intensity in the assembly and prevents the application of the technology on unmanned spacecraft, especially on high orbits. Different approaches to robotic assembly are discussed in [3][4][5][6][7][8]. In these research, a number of issues are investigated, such as accurate placement of the assembled part or unit, reliable fixation, structure scalability, and easy handling of parts with robotic grippers. Besides, another important issue is the coupling (mutual influence) of the robot motion with spacecraft motion, which was investigated in articles and experiments on on-orbit

servicing [9][10][11][12][13]. Recently, researchers have also paid attention to the relatively low stiffness of the space-assembled structures, which translates into the need to consider the natural oscillations of the assembled truss when the robot moves [14]. Application of robotics in projects of in-orbit assembly as well as on-orbit servicing is commonplace nowadays, an example can be seen in [15].

In addition to the abovementioned challenges, it is desirable to provide geometry repeatability during the assembly of large-scale structures for two reasons. First, such structures are often used as support for precise instruments like radio-reflectors or arrays of optical sensors. Second, the deviations from the nominal shape of long structures disturb the spacecraft balance and lead to excessive workload for the reorientation system. Most proposals for robotic assembly involve the fixation of connections by locks that necessarily works with backlash. Taking into account that there are a lot of connections in the structure, the total backlash may reach substantial levels.

In its entirety, assembly technology comprises the following components:

- Assembly robot
- Connection part
- Standard construction parts
- Assembly tools
- Control algorithms of robotic arms for the task of installing a new part
- Control algorithms for robot motion across the structure.

2. Description of assembly technology components

2.1. Connection part

A simple idea of connection is proposed in [16,17], which is to fuse two concentric rings made of low-melting metal that are located in the grooves of the peg and the sleeve. The connection forms when these rings solidify being fused into one. This ring works as a locking element. We have reworked the connection from [17] in order to increase manufacturability and reduce size. The resulting connection has several advantages in terms of robotic assembly [18]. The connection does not require effort to perform assembly (the resistance force during assembly does not exceed 16 N), and the assembly is done in one motion. The locking element does not contain any moving parts, which provides its high reliability. The connection is formed in a way that provides a specific feature, which is the total absence of play in the axial direction. At the same time, load capacity is very high, especially with respect to small size and weight (1200 N tensile load for 12 g weight). Also, the time to perform the connection is small, and the application of forced ventilation will allow for further shortening the duration several times. The absence of solder and main metal adhesion makes possible multiple assembly and disassembly without the loss of solder. Design features and test results are presented in [19] and omitted here. The structure of the connection is clear from Fig. 1. The spring that the unit contains allows assembly from two initial states: when the outer cone is shifted backwards and when the outer cone is situated, such as after the fixation of the connection. In return, it makes it possible to assemble closed structures like triangles (statically indeterminate).

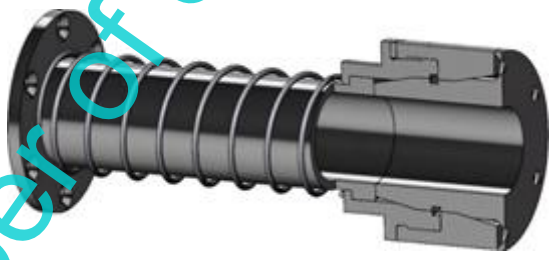

Fig. 1. Standardized connection for robotic assembly

2.2. Standard construction part

Rods and plates are widespread examples of standard construction parts. The proposed robots capable of motion across the spacecraft structure usually employ two types of attachment to the structure. The first type is represented by specialized attachment sites adapted to the robot gripper (rigging points), while universally applicable structures like handrails belong to the second type. Other types of attachment to the spacecraft structure, like usual rails or even the absence of attachments, can be found in the literature but are scarce, and they have several drawbacks. Handrails are more universal in application but require complicated grippers that reduce the reliability of the assembly robot. Conversely, rigging points, though increasing the weight of the structure, usually keep this increase insignificant, especially for “plate” parts. For rod-type trusses, the most convenient attachment site is a fitting where several rods meet; thus, only 5% to 15% of the fitting mass falls on one rod, depending on the truss structure. In papers [19][20], a method to form carbon panels for solar batteries was proposed that provides high stiffness at a low weight. It is not difficult to modify this method by placing the rigging point fixators into the mold, so the “plate” element can be obtained, that is suitable for the robot to navigate through. The assembly process is shown in Fig. 2.

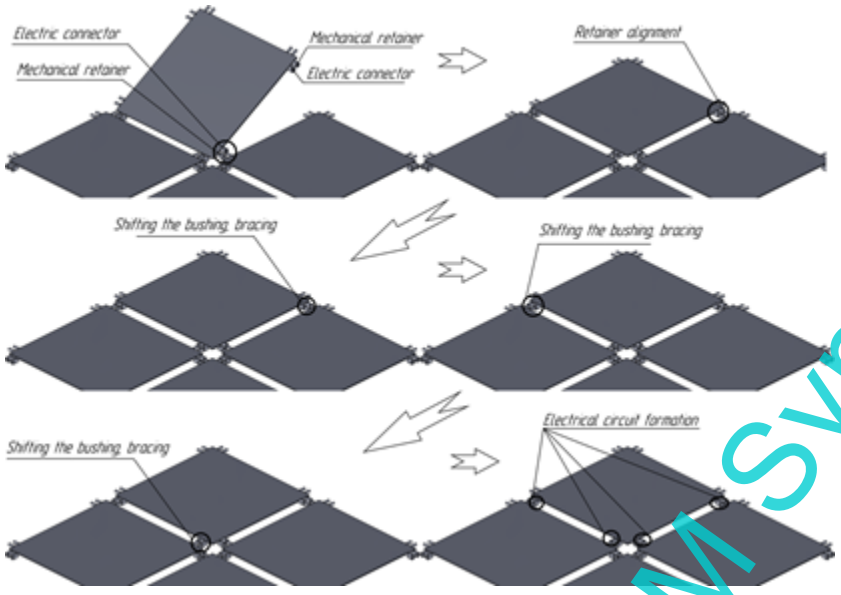

Fig. 2. The assemble process of panel structure

The assembly fitting has two switchable options, which make it possible to install each new assembly part with an arbitrary state of the fitting, either compressed or stretched, while the choice of the option is made by placement of a fixator in the robot gripper. As the assembly fitting allows rotation around its own axis, two fittings can be assembled on one side of the "plate" assembly part. Together with the choice of the fitting option, a two-dimensional structure can be assembled from panels. Truss assembly is performed the same way.

2.3. Assembly tools

The design of the tools for robotic assembly follows the type of connection. As the assembly comprises the melting and solidification of the locking element, the tool must contain a heater and a cooler. The choice from the two connection options is performed before the assembly with the help of a pin actuated by an electromagnet, while the gripper jaws hold the assembly unit. The design of the tool is shown in Fig. 3.

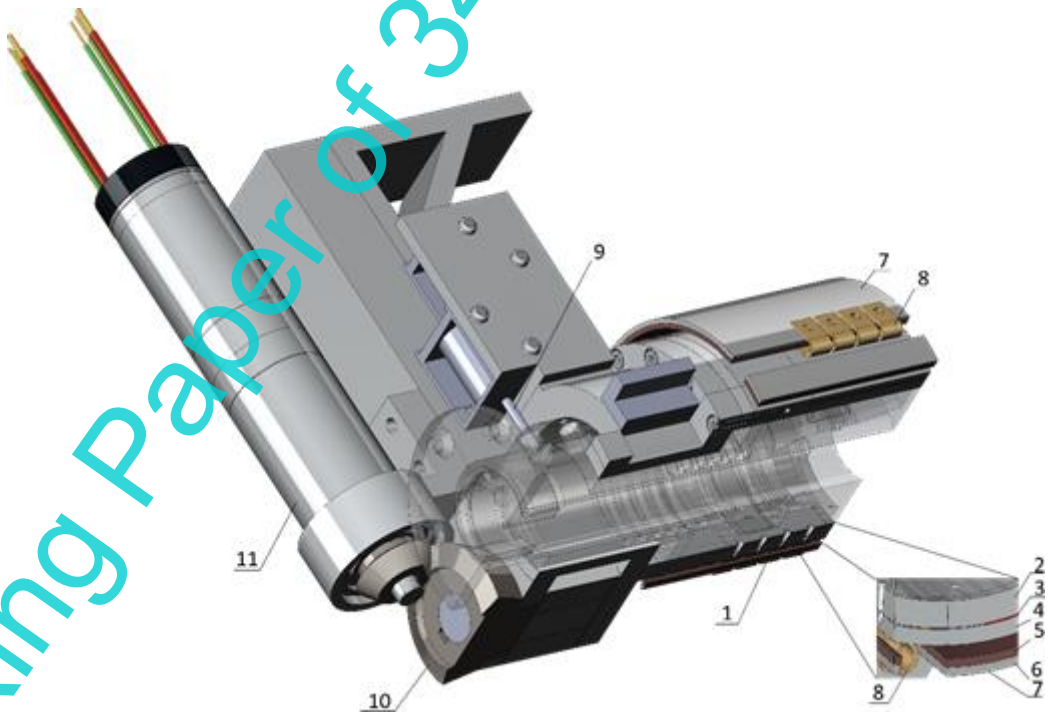

1 – jaw, 2 – load wall, 3 – thin-film heater, 4 – heater clamp, 5 – radiator, 6 – wafer, 7 – MLI, 8 – bimetallic plate, 9 – rod of position choice, 10 – jaws actuator, 11 – electric motor

Fig. 3. General view of the assembly tool

The tool works as follows. Before the assembly starts, the jaws grasp the element to assemble directly at the assembly fitting body, and then the robot performs the preliminary docking. If necessary, the outer bushing of the fitting may be shifted, and the new position is fixed by the rod of position choice. As the fitting is installed in the position for assembly, the heater turns on and the locking rings melt. The end of melting can be deduced from the temperature of the jaws, which only slightly differs from the ring temperature, or by timing, i.e. when the specified time expires. The temperature increase curve has a noticeable break during melting that was captured in the experiment; see Fig. 4. Heating efficiency is increased by the MLI that covers the outer surface of the radiator. This insulation almost totally blocks the heat outflow from the heating area, excluding only heat bridges between the connection element and the structure being assembled. It is assumed to place a heat-insulation spacer made of asbestos-reinforced laminate or ceramics in these areas. As a result of jaws heating-through in bimetallic plates connecting the radiator and the jaws, stresses increase. The radiator is kept from opening by a magnetic latch that releases at the command of the robot, and the radiator flaps open. The inner side of these flaps is covered by thermo-regulating paint (As < 0.2, ε > 0.9), which causes fast cooling of the gripper after the heater turns off. The connection gains strength already when the temperature falls 50 °C below the melting point, therefore, at this moment the gripper can be opened and removed, and further cooling takes place in the structure. When the gripper is sufficiently cooled, bimetallic plates close the radiator flaps back, which are latched by turning on the electromagnet.

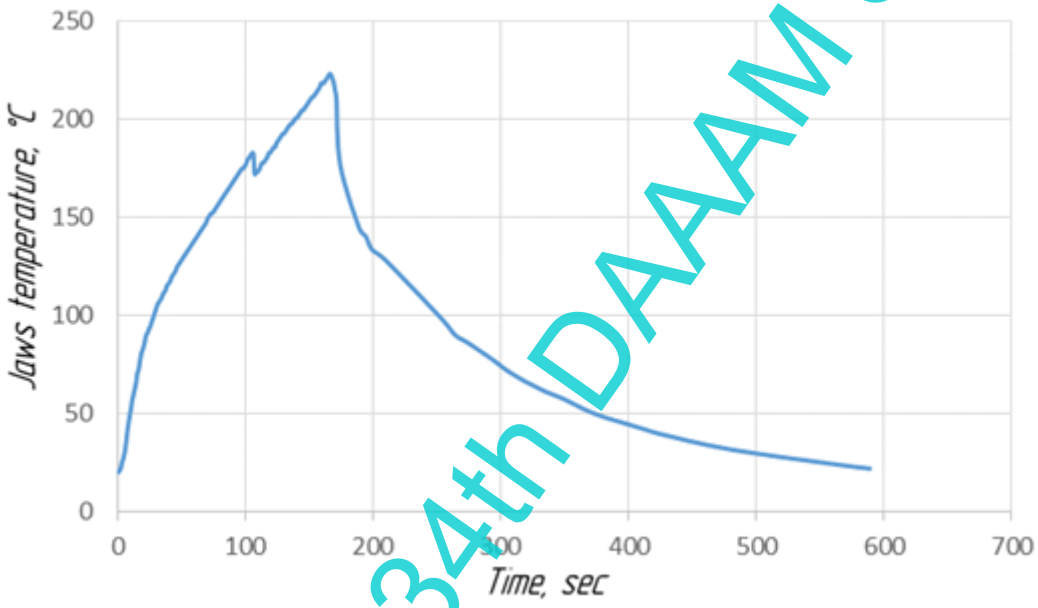

Fig. 4. Temperature of the jaws in the experiment

2.4. Assembly robot

The robot must be capable of performing the following tasks:

- Navigate through the assembled structure
- Carry construction parts, withdrawing the new ones from the warehouse on the servicer spacecraft if necessary
- Perform assembly operations using appropriate tools.

It is also desired that robot should assist in receiving cargo with assembly parts if they are delivered in orbit by a separate launch, i.e. by helping to perform docking of the cargo bay with the servicer spacecraft.

The robot is equipped with a rigging tool as an end-effector to conduct locomotion tasks. It seems complicated to fix the robot on the assembled structure with assembly tools because the jaws of the tool are designed to firmly hold the relatively low weight of one assembly part, not the robot itself. However, the rigging tool can be manufactured in a single package with the assembly tool, so the robot does not need to interchange tools at all.

During the assembly process, the robot must accurately place the assembling part while at the same time compensating for the impact from docking. A joint capable of precise tracking of output angle as well as output torque is the most suitable for this task. It is also desired that the physical stiffness of the joint be substantially lower than the stiffness of the objects with which the robot interacts. The element with low stiffness represents mechanical capacity. Actually, if we introduce a reciprocal to the stiffness quantity, which is compliance p, then the dynamics equation neglecting friction can be written down as

$$m\ddot{x} + \frac{1}{p}x = 0 \tag{1}$$

where x is the generalized coordinate of motion and m is the measure of inertia (mass of moment of inertia).

This equation corresponds to the equation of current in the circuit with capacity p and inductance m. Thus, the increase in compliance has the same effect as the introduction of capacity into an electric circuit, i.e. it provides filtering of low-frequency oscillations, smooths shock impacts, and allows energy storage. The type of joints that contain a compliant element at the output of the gearbox is now known as series elastic actuators (SEA) [21]. The assembly robot should be based on these joints in order to fulfill its purpose.

The joint controller employs measurements from two position sensors: a Hall array on the motor shaft and an optical sensor on the joint output shaft. Due to low backlash as well as high stability of the ratio of harmonic drive, the rotation angle of the gearbox slow shaft is equal with high accuracy to the rotation angle of the motor divided by the gear ratio. Consequently, the measurement error for this angle is equal to the Hall array accuracy divided by the gear ratio as well. By comparing the indirectly measured rotation angle of the gearbox slow shaft with the actual joint output rotation angle and multiplying the difference by the known joint stiffness, one can obtain the external torque applied to the joint. The shape of the elastic element can be designed following different approaches to torsion spring development [22][23][24] [25].

The assembly robot comprises two robotic arms, a base unit, and a vision unit. Each of the arms consists of seven modular joints of three different sizes. A support-bracket with a rigging tool that represents a construction parts magazine is mounted on the base unit. Since construction parts should be equipped with rigging points required for robot motion, it seems most convenient to mount them by rigging point. Before assembly starts, the robot chooses the position to perform it and takes the necessary part from the magazine with the help of the assembly tool.

3. Robotic arm operations during assembly

The vision unit provides lighting for an assembly site as well as the initial orientation of the assembly robot on the basis of the position of tags situated on the construction parts and read by the unit. This operation is necessary because the absolute position error that is accumulated from the docking point of one arm of the robot to the site of the assembly performed by another arm can reach 10 mm, which prevents the mating of lead-in elements of construction parts. By measuring the actual robot pose and the coordinates of the assembly site, the uncertainty can be reduced to 1-2 mm, so it becomes possible to realize preliminary docking followed by alignment along the conical surfaces of the connection parts. The alignment is performed in impedance mode, i.e. the robotic arm intends to minimize the reaction of the support part in the direction orthogonal to the supposed docking axis while moving the tool along that direction, correcting the estimated position of the docking axis based on the reaction force feedback. When the docking is finished, the resistance force starts to grow sharply due to the contact of the peg with the bottom of the conical funnel of the unit. Fig. 5 shows the force portrait measured in the experiment.

The curve in Fig. 5 does not show the growth of force after the assembly has been performed because the experiments were stopped as soon as the funnel bottom was reached; the growth of force then was almost instantaneous and therefore not of interest. The experiments were held in imitation of the impedance mode, i.e. the assembly unit was fixed in a chuck, providing compliant centering and alignment. The chuck was set to move slowly and uniformly in a vertical direction, while the projection of reaction force onto the axis of the fixed part of the connection was logged by a dynamometer. The obtained dependence has three characteristic areas: a gradual increase in reaction force in the process of initial alignment, “a shelf” during the alignment of cylindrical parts, and an abrupt fall when the alignment has been reached. The reaction force in the first area of the curve is defined by the combination of the friction between the peg and the sleeve and the projection of the reaction force of the sloped surface onto the docking axis, and initially the latter part prevails. The main cause of the constant-force area is the friction that is the result of the peg-sleeve misalignment. This misalignment becomes possible due to axial clearance in the H/h fit of the connection, and the primary cause is the noncentrality of the initial contact. After the moment when a substantial part of the connection is centered by the cylindrical surfaces of the peg and the sleeve, the only resistance force becomes the peg-sleeve friction that is caused by the weak preload of the peg by the compliant alignment system. This preload force is much less than the reactive force of the peg-sleeve elastic deformation during alignment, so the resistance reduces sharply. As the experiment results show, the force portrait can be quite accurately approximated by a piecewise linear function, which is employed by the assembly robot to control the performance of the task.

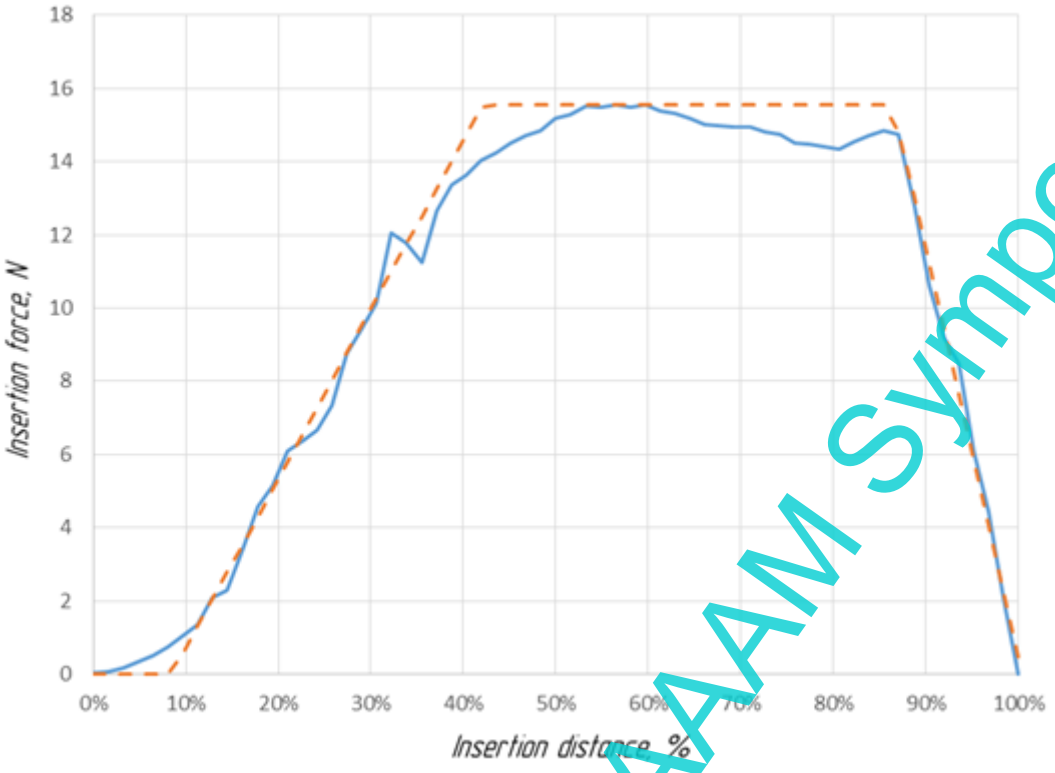

Fig. 5. Contact force during assembly process

The abrupt fall of the resistance force on the last area of the curve becomes possible only in the case of the assembly of a statically determinate structure. In practice, such structures only exist as an intermediate stage of the full assembly process. Installing the closing fitting in a statically indeterminate structure creates forces that are caused by the elastic deformation of the construction part, which results from errors in the installation of the fittings into the structure. These forces depend not only on the peg and sleeve production quality but also on the stiffness of the construction part. The force portrait distorts in this case and depends on the combination of the peg and sleeve tolerance zones. Since it is more convenient to change the shaft tolerance, it is assumed that the sleeve tolerance zone is always H7 (ISO), while the tolerance zone for the cylindrical part of the peg is varied. The resulting force portraits are shown in Fig. 6.

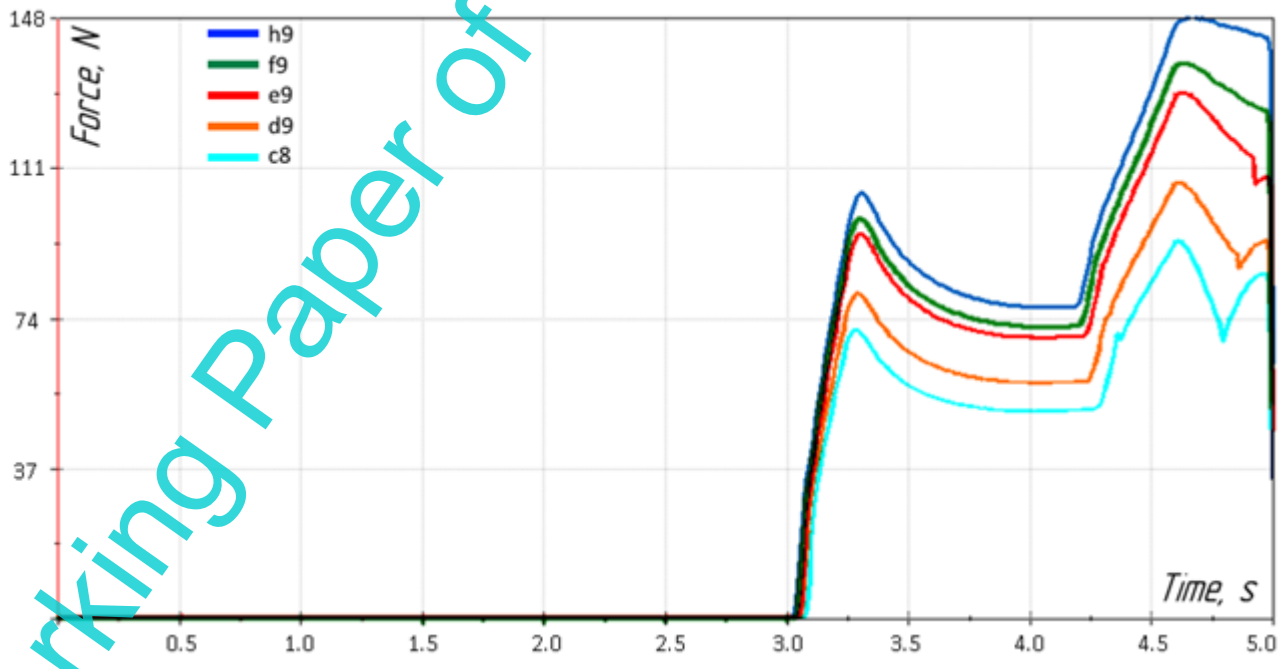

Fig. 6. Contact force during the assembly in a statically indeterminate case

In the statically indeterminate case, the connected parts tend to align not along the common axis but in some random direction that depends on the direction of the accumulated production error. At the same time, when cylindrical parts are mating, the reaction force component caused by the sleeve wall is zero, as in the case of a statically determinate structure, so the overall nature of the load change remains the same on the first two docking stages. However, after the final alignment of the cylindrical parts, the friction force grows rapidly as its cause is not the weak preload (or, in other words, a small transverse force at the robotic tool), but a significantly higher elastic force from the structure deformation. An increase in the guaranteed clearance (see Fig. 6) reduces internal stresses along with the maximal value of the reaction force during docking. This, however, reduces the accuracy of the structure because the uncertainty caused by the random combination of clearances grows. This effect can be lowered if we first assemble the structure on Earth, then mark the parts and assemble them in orbit in the same manner, reproducing the same structure. As a result, the backlash will be zero, and the combination of clearances will be repeated with high accuracy, providing high repeatability if not absolute accuracy. If necessary, the resulting absolute errors can be compensated either mathematically (compensation matrix for orientation) or mechanically by the introduction of a special adjustment platform, whose geometry is again known from the on-ground assembly testing.

4. Control algorithms for robot motion across the structure

Motion of the assembly robot across the assembled structure causes oscillations of this structure and angular momentum variation of certain parts, e.g. the main unit with orientation sensors and the guidance system of the spacecraft. This is associated with mass redistribution and the motion itself. The influence of the change in structure configuration as well as cooperative and uncooperative docking has been considered in many papers [15], [26][27][28][29].

When the assembler moves and construction parts of the structure are carried over, the angular momentum of the whole spacecraft remains constant; however, the angular momentum of certain parts changes, which is due to the variation of the mass distribution across the spacecraft along with the energy introduced into the system by the assembler. The spacecraft is controlled by angular velocity and position, which are determined by instruments located on the base structure, and these quantities do not coincide with those of the inertia ellipsoid of the spacecraft. At the same time, the tidal torque, which is defined by the position of the inertia ellipsoid with respect to orbit, is crucial for stretched spacecraft. As a result, the control system incorrectly compensates for disturbances or even starts such compensation when there are none.

In order to avoid such parasitic compensations, the contribution of the assembler to angular momentum variation should be as low as possible and zero on average. As simulation results show, this condition almost holds for a robot moving human-like when robotic arms move in parallel planes as human legs do. The speed of a distal point (known as the tool center point) for this motion should change in accordance with a trapezoidal law. The estimation of the angular momentum distribution of the subsystem “robot-construction part” for the particular case of motion across the assembled truss is shown in Fig. 7. In simulation, a robot with a total mass of 175 kg and a joint speed limit of 30 °/s was employed. It is clear that variation in angular momentum can be substantial, but the average value is close to zero, which is also the most probable. The deviation of the average value from zero is caused by the inertia variation in the assembly process. The major finding from this estimation is that an assembler robot of about 200 kg is proportionate for a spacecraft of 2000 kg and more because the control system of such a spacecraft is capable of compensating disturbances due to robot locomotion [30].

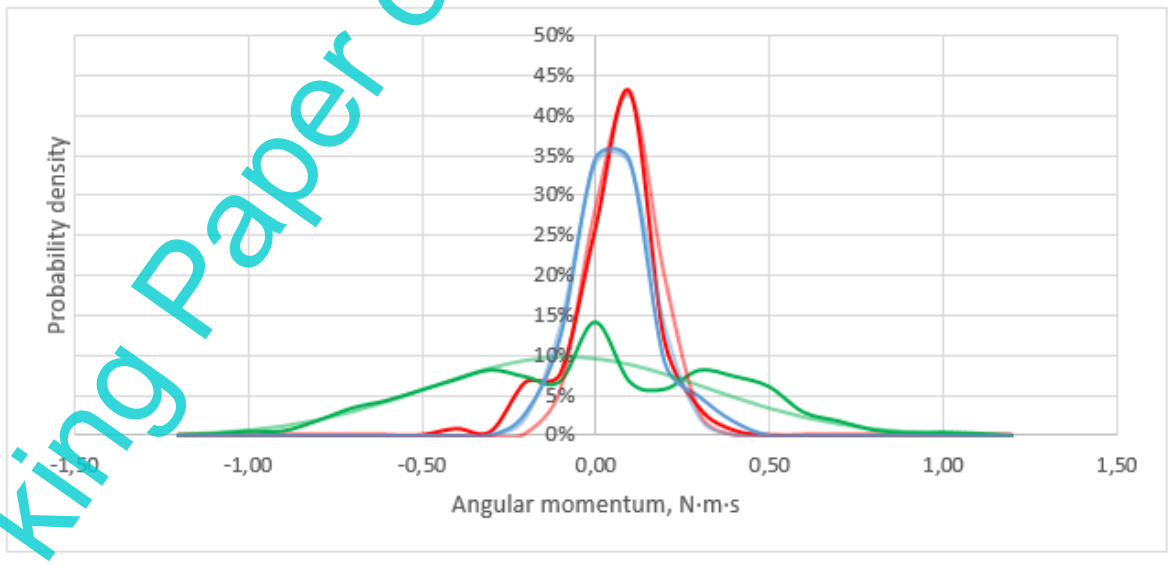

Fig. 7. Angular momentum distribution for locomotion of the assembly robot.
Projections on coordinate axes: OX – red, OY – green, OZ - blue

Locomotion of the robot across the assembled structure involves another issue, which is the unavoidable oscillations of the structure caused by the robot at the time of grasping and releasing the rigging point. Eigenfrequencies of significantly stretched objects like reflectors or solar panels are in the range up to 10 Hz, which means that resonance is possible with the frequencies of the motion control system. Measures directed to avoid this resonance (frequency separation) are ineffective in the case of assembled spacecraft because the eigenfrequency of the structure changes in the process of assembly. Properly coupled performance of the assembler robot and the spacecraft can be guaranteed by damping the arising oscillations through energy dissipation in the motors of the robotic arms. Physically, the damping happens in the course of turning the energy of structure oscillations into the elastic potential energy of the torsion springs in robotic joints, which is further dissipated by activating the generator mode of a brushless electric motor actuating the joint.

Implementation of the latter control mode and its simplification were presented in [31] and [32], respectively. Since the coupling of a robotic arm with an elastic truss is a more complex system than a single loaded elastic joint, it is expected to see some effects in the operation of the system that haven't been observed in [31][32] and are analogous to them. The study of this dynamical system is by itself a topic for an article; however, the overall approach to building a model is rather concise.

The dynamics of the host spacecraft are described by the equation of rotational motion of a rigid body along with an appropriate kinematics relation:

$$\boldsymbol{J}\dot{\boldsymbol{\omega}} + \boldsymbol{\omega} \times (\boldsymbol{J}\boldsymbol{\omega}) + \dot{\boldsymbol{J}}\boldsymbol{\omega} = \boldsymbol{T_R} \tag{2}$$

$$2\dot{\Lambda} = (\Lambda \circ \boldsymbol{\omega}) \tag{3}$$

where J is the spacecraft inertia tensor, ω is the spacecraft angular velocity, and Λ is the quaternion of spacecraft orientation in an inertial system. Rigid-body approximation is justified in this case as variation in the inertia tensor due to oscillations is irrelevant in size and time, resulting in zero contribution taking average over time. Oscillation equations in generalized (modal) coordinates can be written as

$$L_n^T \widehat{M}_{\Sigma_n} L_n \ddot{\xi}_n + L_n^T \widehat{N}_{\Sigma_n} L_n \dot{\xi}_n + L_n^T \widehat{K}_{\Sigma_n} L_n \xi_n = L_n^T \hat{Q}_n \tag{4}$$

where n is an index of the truss component, ξ_n is a vector of generalized coordinates, L_n is a transformation matrix between independent and dependent variables, $\widehat{M}_{\Sigma_n}$ is the inertia matrix, $\widehat{K}_{\Sigma_n}$ is the stiffness matrix, and $\widehat{N}_{\Sigma_n}$ is the damping matrix defined as:

$$\widehat{N}_{\Sigma_n} = \alpha \widehat{M}_{\Sigma_n} + \beta \widehat{K}_{\Sigma_n} \tag{5}$$

where α, β are scalar Rayleigh damping coefficients for truss material.

The vector of generalized forces Q is defined as follows:

$$\hat{Q}_n = L_n^T T_{CBn}^T F_n^f \tag{6}$$

where T_{CB} is the transformation matrix for the Craig-Bampton method [33], and F_n^f is the vector of forces in the component.

Matrices of inertia, stiffness, and damping are determined through the direct stiffness method [34]. Equation (6) can be inverted to find the actual force vector at the reference point. To achieve this, trusses are broken into n components when being reduced, and each of them contains a rigging point. The rigging point is then chosen as the interface point for the reduction of stiffness and inertia matrices. Resulting forces are fed to the input of the dynamic model of the robotic arm equipped with the damping controller, which closes the model.

5. Conclusion

In this paper, implementation issues of robotic assembly of space structures have been considered, which include the design of simple and reliable mechanical connections, algorithms of robotic assembly, oscillation damping, and contact force minimization. The appropriate solutions were formulated, in particular, the physics of the development process of the proposed mechanical connection were studied, and the design of both the robot assembler and the assembled structure was manifested. It was concluded that in order to provide adequate performance of the system, it is necessary to analyze the coupled dynamics of the robot and the structure, assuming controllability of the servicer spacecraft and employment of the damping controller for robot joints. It is expected that the application of SEA joints in the robotic arms of the assembler should solve the main problems arising during the assembly of large-scale non-rigid (compliant) structures. The mathematical model of the coupled robot-structure dynamics was obtained and presented, and our future plans involve a simulation study of the system as well as thorough design and validation of the combined control system of the robot and the spacecraft.

6. Acknowledgments

The work was supported by the Ministry of Science and Higher Education of the Russian Federation. State assignment 075-01595-23-01 “Large-sized space structures assembly methods and technologies research” (FNRG-2022-0007, ID 1021060307686-0-2.2.2).

7. References

[1] https://spacecraftearth.com/portfolio/iss-integrated-truss-structure/, (2017). ISS Integrated Truss Structure, Accessed on: 2023-07-18

[2] Trusov, S.N. & Chernyavskiy, A.G. (1996). “Opyt primeneniya splavov s effectom formy pri sooruzhenii krupnogabaritnykh konstruktsyi v otkrytom kosmose”, Journal of Technical Physics, Vol. 66, No. 11 (in Russian)

[3] Doggett, W. (2002). Robotic assembly of truss structures for space systems and future research plans, Proceedings of IEEE Aerospace Conference, 9-16 March 2002, Big Sky, MT, USA

[4] Jenett, B.; Cellucci, D. & Cheung, K.C. (2015). SpRoUTS (Space Robot Universal Truss System): Reversible Robotic Assembly of Deployable Truss Structures of Reconfigurable Length, Proceedings of AIAA Space 2015 Conferences and Exposition, 31 Aug-2 Sep 2015, Pasadena, California

[5] Hoyt, R.P.; Slosad, J.T. & Moser, T.J. (2016). In-Space Manufacturing of Constructable™ Long-Baseline Sensors using the Trusselator™ Technology. Proceedings of AIAA SPACE 2016. 13-16 September 2016, Long Beach, California

[6] Patane, S.C.; Schomer, J.J. & Snyder, M.P. (2018). Design Reference Missions for Archinaut: A Roadmap for In-Space Manufacturing and Assembly. Proceedings of 2018 AIAA SPACE and Astronautics Forum and Exposition. 17-19 September 2018, Orlando, FL

[7] Wong, I.; Chapin, W. & Komendera, E. (2018). Validation of Operations for the In-Space Assembly of a Backbone Truss for a Solar-Electric Propulsion Tug. Proceedings of 2018 AIAA SPACE and Astronautics Forum and Exposition. 17-19 September 2018, Orlando, FL

[8] Schervan, T.A.; Kortmann, M.; Kai-Uwe Shronder, P. & Kreisel, J. (2017). iBOSS Modular Plug & Play - Standardized Building Block Solutions for Future Space Systems Enhancing Capabilities and Flexibility, Design, Architecture and Operations. Proceedings of 68 International Astronautical Congress. Adelaide, Australia, 25-29 September 2017

[9] Shah, S. V.; Sharf, I. & Misra, A. (2013). Reactionless path planning strategies for capture of tumbling objects in space using a dual-arm robotic system. Proceedings of AIAA Guidance, Navigation, and Control (GNC) Conference (p. 4521)

[10] Kasai, T.; Oda, M. & Suzuki, T. (1999). Results of the ETS-7 mission - rendezvous docking and space experiments. Proceedings of 5th International Symposium on Artificial Intelligence, Robotics and Automation in Space (i AIRAS), Noordwijk, Netherlands, 1999

[11] https://www.nasa.gov/pdf/167813main_RP-06-119_05-020-E_DART_Report_Final_Dec_27.pdf, (2006). NESC Review of Demonstration of Autonomous Rendezvous Technology (DART) Mission Mishap Investigation Board Review (MIB). Accessed on: 2023-07-18

[12] Dennehy, C. J. & Carpenter, J. R. (2011). A summary of the rendezvous, proximity operations, docking, and undocking (rpodu) lessons learned from the defense advanced research project agency (darpa) orbital express (oe) demonstration system mission (No. NESC-RP-10-00628).

[13] Henshaw, C. G. (2014). The darpa phoenix spacecraft servicing program: Overview and plans for risk reduction. Proceedings of International Symposium on Artificial Intelligence, Robotics and Automation in Space (i-SAIRAS). European Space Agency.

[14] Yuchen She, Shuang Li, Yufei Liu, Menglong Cao, "In-orbit robotic assembly mission design and planning to construct a large space telescope," J. Astron. Telesc. Instrum. Syst.

[15] Lopota, A.; Dalyaev, I.; Shalyko, I.; Kuznetcova, E. & Belezyakov, I. (2016). Means of robotic support for on-orbit servicing. Proceedings of the 26th DAAAM International Symposium (pp. 0865-0870). 2016.

[16] Pochezhertsev, A. G. & Kopylov V. M. (2020). Universal Docking Assembly Design for Automatic Assembly of Large Untight Structures in Near-Earth Space. Proceedings of 2020 International Conference on Industrial Engineering, Applications and Manufacturing (ICIEAM). – 2020. – pp. 1-6

[17] Kopylov V.M. & Pochezhertsev A.G. (2023). System for robotic assembly of large-sized trusses, including on earth's orbit or moon. Patent RU2790311C2.

[18] Kopylov, V. M. & Volnyakov K.A. (2022). Малогабаритные средства адаптации КА для возможности робототехнического обслуживания на орбите. (Small-size Means of Adaptation of Spacecraft for On-orbit Servicing Capability, in Russian). Proceedings of XIV Open Russian Scientific and Technical Conference “Robotics and Artificial Intelligence” (RAI) – 2022. – pp. 37-42

[19] Drondin, A.V.; Zernov, O.D. & Yanchur, S.V. (2017). Manufacturing method of celled honeycomb filler from composite materials. Patent RU2623781C2.

[20] Rebrov, S. G.; Yanchur, S. V.; Drondin, A. V. & Zernov, O. D. (2019). “Developing the concept of solar energy units robotic assembly in orbit”, Aerospace MAI Journal, Vol. 26, No. 1, pp. 201-211

[21] Pratt, G A. & Williamson, M.M. (1995). Series elastic actuators. Proceedings of 1995 IEEE/RSJ International Conference on Intelligent Robots and Systems. Human Robot Interaction and Cooperative Robots. Vol. 1. IEEE, 1995.
[22] Carpino, G.; Accoto, D.; Sergi, F.; Tagliamonte, L.N. & Guglielmelli, E. (2012). "A novel compact torsional spring for series elastic actuators for assistive wearable robots", Journal of Mechanical Design, Vol. 134, No.12
[23] Tagliamonte, N. L.; Sergi, F.; Carpino, G.; Accoto, D. & Guglielmelli, E. (2010). Design of a variable impedance differential actuator for wearable robotics applications. Proceedings of 2010 IEEE/RSJ International Conference on Intelligent Robots and Systems (pp. 2639-2644). IEEE.
[24] Zhou, M. (2021). "A method to determine the topology of custom torsional elastic element for the lightweight rotary series elastic actuator", Journal of Physics: Conference Series, Vol. 1939, No. 1, IOP Publishing
[25] Diftler, M. A.; Mehling, J. S.; Abdallah, M. E.; Radford, N. A.; Bridgwater, L. B.; Sanders, A. M.; ... & Ambrose, R. O. (2011). Robonaut 2-the first humanoid robot in space. Proceedings of 2011 IEEE international conference on robotics and automation (pp. 2178-2183). IEEE.
[26] Rognant, M.; Cumer, C.; Biannic, J. M.; Roa, M. A.; Verhaeghe, A. & Bissonnette, V. (2019). Autonomous assembly of large structures in space: a technology review. Proceedings of EUCASS 2019.
[27] Fukazu, Y.; Hara, N.; Kanamiya, Y. & Sato, D. (2009). Reactionless resolved acceleration control with vibration suppression capability for JEMRMS/SFA. Proceedings of 2008 IEEE International Conference on Robotics and Biomimetics, pp. 1359-1364. IEEE.
[28] Costa, A.; Abdel-Rahman, A.; Jenett, B.; Gershenfeld, N.; Kostitsyna, I. & Cheung, K. (2019). Algorithmic approaches to reconfigurable assembly systems. Proceedings of 2019 IEEE Aerospace Conference, pp. 1-8. IEEE
[29] Martinez-Moritz, J.; Rodriguez, I.; Nottensteiner, K.; Lutze, J.-P.; Lehner, P. & Roa, M. A. (2021). Hybrid Planning System for In-Space Robotic Assembly of Telescopes using Segmented Mirror Tiles. Proceedings of 2021 IEEE Aerospace Conference, pp. 1-16. IEEE.
[30] Mkrtychyan, A. R.; Bashkeev, N. I.; Yakimovskii, D. O.; Akashev, D. I. & Yakovets, O. B. (2015). "Control moment gyroscopes for spacecraft attitude control systems: Current status and prospects", Gyroscopy and Navigation, Vol. 6, No. 3, pp. 236-240.
[31] Albu-Schäffer, A.; Ott, C. & Hirzinger, G. (2007). "A unified passivity-based control framework for position, torque and impedance control of flexible joint robots", The international journal of robotics research, Vol. 26, No.1, pp. 23-39.
[32] Shardyko, I.; Samorodova, M. & Titov, V. (2020). Development of control system for a SEA-joint based on active damping injection. Proceedings of 2020 International Conference on Industrial Engineering, Applications and Manufacturing (ICIEAM), pp. 1-6. IEEE.
[33] Craig Jr, R. R. & Bampton, M. C. (1968). "Coupling of substructures for dynamic analyses", AIAA journal, Vol. 6, No. 7, pp. 1313-1319.
[34] Felippa, C. A. (2004). Introduction to finite element methods, University of Colorado, T. 885.